



Investigation of nitrogen doped diamond like carbon films as counter electrodes in dye sensitized solar cells

Sea-Fue Wang^{a,*}, K. Koteswara Rao^a, Thomas C.K. Yang^b, Hsin-Pei Wang^a

^a Department of Materials and Mineral Resources Engineering, National Taipei University of Technology, Taipei 106, Taiwan, ROC

^b Department of Chemical Engineering and Biotechnology, National Taipei University of Technology, Taipei 106, Taiwan, ROC

ARTICLE INFO

Article history:

Received 3 November 2009

Received in revised form 9 October 2010

Accepted 21 October 2010

Available online 30 October 2010

Keywords:

Dye-sensitized solar cell (DSSC)

Counter electrode

Diamond-like carbon (DLC)

Cathodic arc deposition

ABSTRACT

The present work mainly deals with the development of nitrogen doped diamond like carbon (n-type DLC) thin films as counter electrode (CE) in place of platinum that is commonly used as a counter electrode and catalyst in the dye sensitized solar cell (DSSC) design. The DLC films were grown on indium-tin-oxide coated glass substrates using cathodic arc physical vapor deposition (PVD). Four different CEs namely, ITO/Pt/DLC (n-type), ITO/Cr/DLC (n-type), ITO/Cr/DLC (n-type)/Pt, and Glass/Cr/DLC (n-type)/Pt apart from standard ITO/Pt are prepared. The surface morphology, sheet resistance and redox catalytic activity for I^-/I_3^- of the above CEs were characterized by scanning electron microscopy (SEM), four point probe resistivity and cyclic voltammetry (CV), respectively. The performance of DSSCs with these DLC based CEs was evaluated by photo electrochemical response, in this study. The CE with a structure of ITO/Cr/DLC (n-type)/Pt (deposition time 10 s), exhibited an efficiency of 3.3%. After replacing ITO glass substrate with simple glass substrate, i.e. for Glass/Cr/DLC (n-type)/Pt structure, the photoelectric efficiency could reach to 3.2%, indicating that we can successfully replace ITO glass substrate with simple glass plate in the present design and retain the conversion efficiency as well.

© 2010 Elsevier B.V. All rights reserved.

1. Introduction

Dye sensitized solar cells (DSSCs) are slated to become one of the cheapest alternatives to conventional p–n junction photovoltaics [1]. Their high energy conversion efficiency, low cost of production and easy methods of fabrication, make them as attractive candidates for next generation of solar cells [2–5]. The DSSC design primarily consists of (i) a dye-covered nanocrystalline TiO_2 layer on a transparent conductive glass substrate as a 'photoanode' (ii) an iodide/triiodide redox couple in an organic solvent as an 'electrolyte' and (iii) a platinized conductive glass substrate as a 'counter electrode'. Under illumination, the dye gets photo-excited and injects the electrons into conduction band of TiO_2 . Later the electrons are collected by the substrate (transparent conducting oxide) and transferred to the counter electrode through external circuit (load). The oxidized dye accepts electrons from the iodide ion (I^-) of redox electrolyte and the resultant tri-iodide (I_3^-) ions are reduced back to I^- at the counter electrode. So the role of counter electrode is to reduce the redox species used as mediator

and thus regenerate the sensitizer (dye) in neutral form. For this a high electrochemical activity of the counter electrode is required along with good conductivity.

In DSSCs, counter electrodes are usually made of conducting glass substrates coated with Pt films. Conversion efficiencies greater than 11% were achieved with Pt as catalyst for counter electrode [6,7]. However, since Pt is relatively expensive and less available, other alternatives are explored for further lowering the overall cost of the solar cell. The counter electrode, in principle, should possess low sheet resistance and high reduction rate (catalytic activity) of redox electrolyte, for improved performance of DSSC. Towards this end, presently, carbon based and conducting polymer based counter electrodes are studied [8]. Many carbonaceous materials like, activated carbon, graphite, carbon nanotubes, fullerenes, etc. have been used as counter electrodes in DSSCs with impressive conversion efficiencies [9]. By employing carbon black as catalyst in the counter electrode preparation, Murakami et al. have obtained a cell efficiency of as high as 9.1% under 100 mW cm^{-2} light intensity [10]. Recently, Ramasamy et al. have reported a maximum energy conversion efficiency of 7.59% for spray coated multi-wall carbon nanotube counter electrode DSSC under similar one sun illumination [11]. Their remarkable electronic conductivity, resistance to corrosion, tri-iodide reduction capability along with fairly low cost and wide availability, makes these carbon based materials a favorable option for counter electrodes. Among the polymer materials for counter

* Corresponding author. Present address: National Taipei University of Technology, Department of Materials and Mineral Resources Engineering, 1, Sec. 3, Chung-Hsiao E. Rd., Taipei 106, Taiwan, ROC. Tel.: +886 2 0919 328 953; fax: +886 2 8773 2608.

E-mail address: seafuewang@yahoo.com (S.-F. Wang).

Table 1
Counter-electrodes and their deposition parameters.

Counter-electrodes and coating parameters	Variable	
Standard: ITO/Pt		
Chamber vacuum is approximately 6–7 Pa, electric current: 30 mA, coating time: 2 min		
(1) ITO/Pt/DLC (n-type)		
Pt film: 1×10^{-2} Torr-100 W-30 sccmAr-2 min	Amount of doped N ₂ is X= 0, 5, 10, 30, 60 sccm	
DLC film: 1000 V-50 A-60 sccm Ar-X sccmN ₂ -1.5 min		
(2) ITO/Cr/DLC (n-type)		
Cr film: 60 V-50 A-60 sccm Ar-1 min	The coating time is changed respectively as X= 5, 10.5, 12 min	
DLC: 100 V-45 A-60 sccm Ar-X min		
(3) ITO/Cr/DLC (n-type)/Pt		
Cr film: 60 V-50 A-60 sccm Ar-1 min	Platinum coating time is X= 5, 10 s.	
DLC film: 100 V-45 A-60 Ar-10 sccm N ₂ -1.5 min		
Pt film: 1×10^{-2} Torr-100 W-30 sccm Ar-Xs	Platinum coating time is X= 2, 3 min	
(4) Glass/Cr/DLC (n-type)/Pt		
Cr film: 60 V-50 A-60 sccm Ar-1 min		
DLC film: 100 V-45 A-60 sccm Ar-10 sccm N ₂ -1.5 min		
Pt film: 1×10^{-2} Torr-100 W-30 sccm Ar-X min		

Note: ITO represents indium-tin-oxide coated glass substrates.

electrodes, the poly (3,4-ethylenedioxythiophene) (PEDOT) doped with p-toluenesulfonate (PEDOT-TsO) needs a mention as it shows a similar electro-catalytic effect for I_3^- reduction to that of Pt deposits [12,13]. Composites of polymers and carbon black also gave interesting results [14,15].

Diamond like carbon (DLC) is another form of meta-stable amorphous carbon with significant proportions of sp^3 type bonds (50–60%) compared to sp^2 or sp carbon and it also contains hydrogen as other element [16]. Their properties are similar to crystalline diamond, i.e. high hardness, chemical inertness, high thermal conductivity, high electrical resistivity, optical transparency, etc. and their band gap can be tuned by manipulating the sp^2 and sp^3 bonding ratio [17,18]. The electrical conductivity of DLC films can be improved by doping with nitrogen [19] to result in semi-conducting to highly conducting behavior [20,21]. DLC films are in use as antireflection and protective coatings of solar cells designed for space [22] while the nitrogen doped DLC films are used in similar p–n junction solar cells or schottky solar cells in combination with p-Si or ITO, respectively [23,24]. In view of these relevant applications of nitrogen doped DLC films in solar cells, we have made attempts to use the same as a possible counter electrode material in DSSCs, as part of our search for alternatives to Pt. Herein we describe the fabrication and testing of four different combinations of nitrogen doped DLC films to act as counter electrodes in the DSSC design.

2. Experimental procedure

2.1. Materials

TiO₂ powder (P25, Degussa), ethanol anhydrous (Aldrich, 99.5%), Triton X-100 (ACROS), acetyl acetone (Aldrich), TiCl₄ (Aldrich, 1 M), acetonitrile (J.T. Baker, HPLC grade), I₂ (Sigma, >95%), LiI (ProChem, 99+ %), poly ethylene glycol (PEG, Showa chemical co Ltd., Japan), electrolyte (solaronix), were used as purchased. ITO (Indoped SnO₂, 8.08 Ω /sq) coated glass substrates were cleaned in isopropyl alcohol, acetone and DI water sequentially by ultrasonic treatment for 20 min each before using.

2.2. Preparation of TiO₂ thin film photoanode

Thin films of porous TiO₂ were deposited on a cleaned ITO glass as follows: 3 g of TiO₂ powder is taken in a container and 1 ml of water, 0.9 g of PEG and 0.1 ml of acetyl acetone are added to it and mixed thoroughly for 20 min. Another 3 ml more of water was added by mixing well after each 1 ml of addition. After adding 0.05 ml of Triton X-100, the container is kept for 24 h in an ultrasonic water bath at 28 °C to get a well-dispersed TiO₂ paste. This paste is spin coated on cleaned ITO substrate (0.5 cm \times 0.5 cm) at 2000 rpm for 5 s and 4000 rpm for 10 s and then dried at 60 °C for 10 min in an oven. TiO₂ is spin coated again at 1000 rpm for 5 s and 2000 rpm for 10 s with subsequent drying at 60 °C for 10 min. The TiO₂ coated ITO is sintered at 450 °C for 30 min. It is finally treated with TiCl₄ solution and dried at 70 °C for 30 min before its being sintered again at 450 °C/30 min.

The TiO₂ film is immersed in 50 ml of 0.5 mM ethanolic N719 (bis (tetrabutylammonium) – cis-bis (thiocyanato) bis (2,2' – bipyridine-4,4'-dicarboxylate) – Ru (II)) dye solution for 24 h in dark at room temperature so that a monolayer of dye is adsorbed and an equilibrium is attained. Later the film is cleaned with ethyl alcohol and dried in an oven for readily using it as a photo anode or working electrode in DSSC.

2.3. Preparation of counter electrodes

The four different counter electrode series apart from the standard ITO/Pt having different layer by layer designs are given in Table 1, along with the deposition parameters for individual layers. They are designated as (i) ITO/Pt/DLC (n-type), (ii) ITO/Cr/DLC (n-type), (iii) ITO/Cr/DLC (n-type)/Pt and (iv) Glass/Cr/DLC (n-type)/Pt. The Pt is deposited by ion sputtering for standard ITO/Pt CE and by RF sputtering for remaining CEs. Cr and nitrogen doped DLC are deposited using cathodic arc physical vapor deposition (PVD) similar to our earlier report [25].

For the standard ITO/Pt CE preparation by ion sputtering, the vacuum of the chamber is adjusted to 6–7 Pa and a current of magnitude 30 mA is used. A layer of 20 nm thick platinum is deposited for a coating time of 2 min. For Pt thin films deposited by radio-frequency (RF) magnetron sputtering, Argon with at least 99.995% pure was used as the working gas. The target size and the power density for RF sputtering are 2 in. in diameter and 4.9 W/cm², respectively. Prior to deposition, the target was sputter-cleaned. Working pressure was maintained at 1.38 Pa (1×10^{-2} Torr) while RF power was 100 W.

For DLC, the target (Graphite) size and the current density for cathodic arc PVD are 1 in. in diameter and 8.89 A/cm², respectively. The arc current was 60 A for Cr and 45 A for graphite. Cr interlayer of thickness 218 nm was deposited first, and then nitrogen doped DLC was coated on the top of the Cr interlayer. The thickness of Pt is controlled by deposition time while the quality and thickness of DLC (n-type) are monitored by the partial pressure of nitrogen during deposition and the time of deposition.

2.4. Characterization of electrodes and the performance of DSSCs

A Hitachi S-4700 field emission scanning electron microscope (SEM) was used to obtain the surface microstructure of photoanode, counter electrode and the thicknesses of different layers by side view SEM image. Sheet resistances of the counter electrodes were measured by the four-point probe method using Mitsubishi Chemical MCP-T610 resistance measurement system. Cyclic voltammetry (CV) was carried out in a three electrode single compartment cell with different DLC based films as working electrodes, Pt foil as counter electrode and an Ag/AgCl as reference electrode, dipped in an acetonitrile solution of 10 mM LiI, 1 mM I₂ and 0.1 M LiClO₄. CV was performed using CH Instruments of electrochemical measurement system with a voltage sweep rate of 0.05 V/s.

Dye sensitization solar cell is assembled by taking a the DLC based counter-electrode and the TiO₂ working electrode and clamping them together with a 1 mm width spacer between them (Solarix Corporation, SX1170) to seal them by heating for approximately 2–3 min (100 °C) that causes thermosetting of SX1170 between the two piece of electrodes. A little amount of electrolyte (50 mM I₂, 500 mM LiI and 500 mM 4TBP (4-tert-butyl pyridine)) is dripped into the cell by a capillary to complete the DSSC configuration. The photo electrochemical characterization of DSSCs was accomplished using an AM 1.5–simulated light irradiation with a 300 W Xe lamp (NEWPORT 66902) as light source and Keithly 2400 as source meter. The incident light intensity and the active cell area were 100 mW cm⁻² and 0.25 cm², respectively.

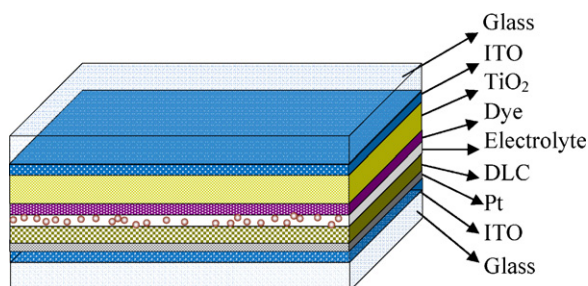


Fig. 1. Structure of assembled DSSC with DLC based counter electrode and other layers.

3. Results and discussion

Thin films of TiO_2 spin coated on ITO are examined by powder XRD & SEM and are found to have a thickness of 12–15 μm with an average particle size of $\sim 20\text{ nm}$. For best results, a minimum TiO_2 thickness of about 10 μm is commonly used in the DSSCs [26] and hence the present films are well suited for use as working electrodes. Apart from the standard ITO/Pt counter electrode, the first type of DLC based counter electrode studied in this work is ITO/Pt/DLC (n-type). The Pt layer (150 nm) deposited by RF sputtering below the DLC (n-type) layer is deliberately chosen to increase the adhesiveness of DLC (n-type) on ITO and also to retain the good conductivity required between DLC (n-type) and ITO. Since a specific doping amount of nitrogen in DLC gives the highest conductivity [20], the concentration of nitrogen is monitored by depositing the DLC (n-type) layer for 1.5 min each with 0, 5, 10, 30 and 60 sccm of N_2 resulting in thicknesses of 165, 165, 198, 199, 165.5 nm, respectively. Hopping conduction is enhanced through N incorporation and the corresponding lattice relaxation. Substitutional N incorporation will compensate the gap states and thus move the Fermi level up towards the conduction-band edge. Moreover, relaxation of the lattice network due to the presence of N will create the gap defect states. N incorporation in DLCs close to existing π bonded sites will lead to graphitization around the N atoms which in turn will trigger increase in the conductivity due to the conduction along π bonded chains [31]. The assembled structure of DSSC with different layers, including the ITO/Pt/DLC (n-type) counter electrode, is shown in Fig. 1.

The I - V curves and photovoltaic parameters of the DSSCs with the ITO/Pt/DLC (n-type) counter electrodes are shown in Fig. 2 and Table 2, respectively. From them, it is clear that standard ITO/Pt CEs (both Ion sputtered and RF sputtered Pt) have good conversion efficiency compared to all other CEs. Since the kind of Pt deposition also usually influences the efficiency of counter electrode [27], the Ion sputtered Pt showed better performance than RF sputtered Pt in the present study. For convenience, the Pt in all the subsequent ITO/Pt/DLC (n-type) and other counter electrodes is deposited by RF sputtering. With the undoped DLC in the counter electrode, the conversion efficiency has decreased to 1.65% from the 3.20% for ITO/Pt electrode. After doping 5 sccm N_2 into DLC there is not much change

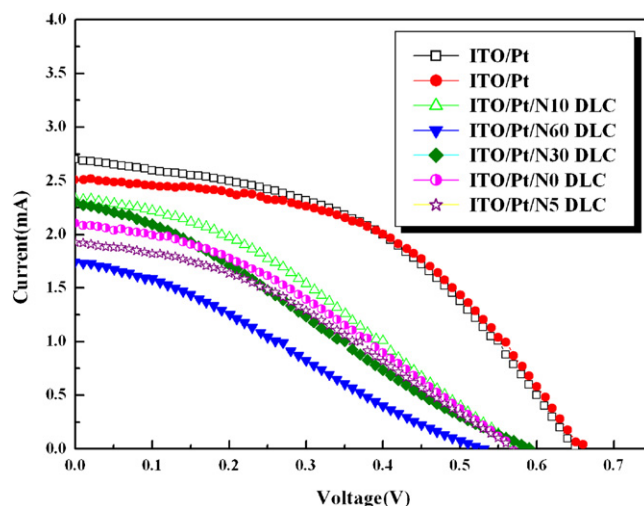


Fig. 2. Current–Voltage curves for various DLC based counter electrodes in DSSC.

in the efficiency but when the nitrogen doping is 10 sccm, the efficiency has improved to 1.85%, which is the best among ITO/Pt/DLC (n-type) counter electrodes studied here. Since doping of more than 10 sccm (both 30, 60 sccm of N_2) resulted in decrease of conversion efficiency, it is considered as an optimum doping level of nitrogen in DLC for good performance in this series of counter electrodes.

When the counter electrode is only ITO glass without any Pt layer on it, the I - V curves and photovoltaic parameters (not presented here) of the cell gave an efficiency of only 0.04% similar to earlier reports [28]. So the need of Pt layer for redox catalysis is clearly evident from the high efficiency (3.20%) of ITO/Pt counter electrode in the cell. Now, when a layer of nitrogen doped DLC is deposited the Pt layer is not completely available for contributing to the catalytic activity of redox reactions. Therefore, with 1.85% conversion efficiency, the ITO/Pt/DLC (n-type) counter electrode with 10 sccm of doped nitrogen has definitely shown a certain catalytic activity towards the reduction of I_3^- to I^- . Though the fill factor (FF) was constant up to 10 sccm of N_2 doping concentration, the short circuit current (I_{sc}) was high for 10 sccm N_2 doped DLC and also there is not much variation in the open circuit voltage (V_{oc}) for 5–30 sccm N_2 doped DLC counter electrodes.

The high conductivity of 'ITO/Pt/10 sccm N_2 doped DLC' electrode is also understood from the sheet resistivity data given in Table 3. For the standard counter electrode ITO/Pt and the 0, 5 sccm N_2 doped DLC based CEs, the resistivity lies in 1.4–1.5 Ω/sq . When the nitrogen doping is increased to 10, 30 sccm in DLC, the resistivity decreases to 1.38 and 1.34 Ω/sq , respectively. This low sheet resistance of 'ITO/Pt/10 sccm N_2 doped DLC' has contributed to its better conversion efficiency. Though the sheet resistivity of 'ITO/Pt/30 sccm N_2 doped DLC' is still less, the catalytic activity of it might be different and therefore 'ITO/Pt/10 sccm N_2 doped DLC' showed superior performance in conversion efficiency. To understand the electro catalytic activity of counter electrodes towards

Table 2
Photovoltaic parameters of DSSCs using ITO/Pt/DLC (n-type) as counter-electrodes.

Counter-electrode	Short circuit current I_{sc} (mA)	Open-circuit potential V_{oc} (V)	Fill factor (FF)	Conversion efficiency (η)
ITO/Pt (RF sputtered)	2.70	0.65	0.46	3.20%
ITO/Pt (Ion sputtered)	3.14	0.65	0.43	3.53%
ITO/Pt/0 sccm N_2 doped DLC	2.10	0.57	0.34	1.65%
ITO/Pt/5 sccm N_2 doped DLC	1.92	0.57	0.34	1.55%
ITO/Pt/10 sccm N_2 doped DLC	2.33	0.58	0.34	1.85%
ITO/Pt/30 sccm N_2 doped DLC	2.29	0.59	0.29	1.49%
ITO/Pt/60 sccm N_2 doped DLC	1.74	0.53	0.29	1.07%

Note: ITO represents indium-tin-oxide coated glass substrates.

Table 3
Sheet resistivity of counter-electrodes ITO/Pt/DLC (n-type).

Counter electrode	Sheet resistivity (Ω/sq)
ITO/Pt (standard cell)	1.50
ITO/Pt/0 sccm N_2 doped DLC	1.47
ITO/Pt/5 sccm N_2 doped DLC	1.53
ITO/Pt/10 sccm N_2 doped DLC	1.38
ITO/Pt/30 sccm N_2 doped DLC	1.34
ITO/Pt/60 sccm N_2 doped DLC	1.58

Note: ITO represents indium-tin-oxide coated glass substrates.

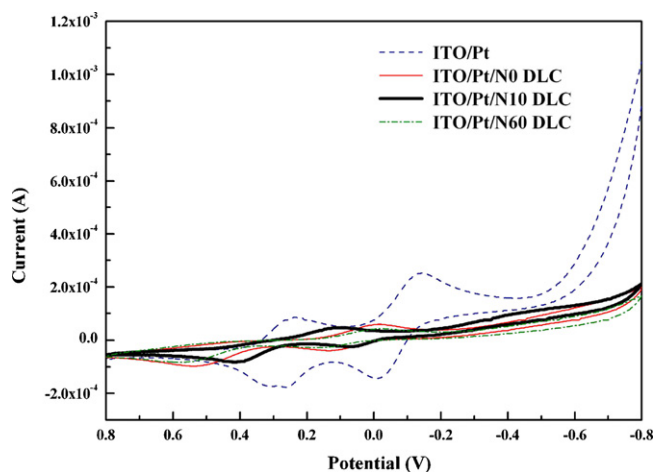


Fig. 3. Cyclic voltammograms for the ITO/Pt, ITO/Pt/N0-DLC (0 sccm N_2), ITO/Pt/N10-DLC (10 sccm N_2) and ITO/Pt/N60-DLC (60 sccm N_2) electrodes.

$\text{I}_2 + \text{I}^-$ system, cyclic voltammograms are recorded in the potential range of -0.8 to $+0.8$ V with a scan rate of 0.05 V and the corresponding plots are presented in Fig. 3.

For convenience and comparison, cyclic voltammograms of only the standard ITO/Pt and 0, 10, 60 sccm of N_2 doped DLC based counter electrodes are presented in Fig. 3. A pair of oxidation (anodic) and a pair of reduction (cathodic) peaks are observed for all the electrodes. When the potential is swept from the positive to negative value, reduction of I_2 to I_3^- (b') and I_3^- to I^- (b) occur by reactions (1) and (2), respectively [29].



In the reverse sweep, i.e. from negative to positive potential, oxidation of I^- to I_3^- (a) and I_3^- to I_2 (b) occur sequentially corresponding to reactions (2) and (1) in the reverse process. Both the anodic and the cathodic peaks are large and wide (in terms of peak height and area under the peak) for the ITO/Pt counter electrode compared to other DLC based electrodes. This indicates a high catalytic activity of ITO/Pt for reduction of I_3^- and oxidation of I^- in comparison to other electrodes. However, for the DLC based electrodes both the peak heights and the areas are smaller compared to ITO/Pt. The peak potentials usually give information about the kinetics of oxidation (a, a') and reduction (b, b') processes occurring

at the electrode while the peak current (peak height) gives information about concentration and stability of redox species. Among the DLC based electrodes, the 'ITO/Pt/10 sccm N_2 doped DLC' showed least positive peak potentials and more peak height compared to others, hence resulting in superior performance within them. This has contributed to its better conversion efficiency along with its good conductivity.

The optimal doping of nitrogen in DLC has been assessed in the first series of counter electrodes, ITO/Pt/DLC (n-type), with 10 sccm of N_2 showing the best conversion efficiency. In the second series of counter electrodes, the optimal thickness or deposition time of 10 sccm nitrogen doped DLC is studied. For this series, instead of Pt layer a 218 nm Cr layer is deposited by cathodic arc PVD in its place for cost reduction and better adhesion of DLC layer to ITO. Three counter electrodes of ITO/Cr/N-doped DLC structure are prepared with the deposition times of N-doped DLC as 5, 10.5 and 12 min to result in thicknesses of 62.5, 125 and 131 nm, respectively.

The photovoltaic performance of these counter electrodes is assessed and their corresponding parameters including conversion efficiency are presented in Table 4. Among the three DLC based CE, the one with N-doped DLC of 10.5 min deposition time, has shown better conversion efficiency of 1.57% while the other two have still low efficiency. The overall performance is also lower than the first series of counter electrodes with Pt as interlayer between ITO and N-doped DLC. This could be due to the better conductivity of Pt compared to Cr and also due to platinum's partial contribution to redox catalytic activity. The sheet resistivity values of three counter electrodes, with deposition times of 5, 10.5, 12 min for N-doped DLC are 7.73, 7.59 and 7.90 Ω/sq , respectively. These values are nearly 5 times more than the resistivities for first series of counter electrodes (Table 3) with Pt as inter layer. The cyclic voltammograms for the three electrodes (not presented here) also showed small peak currents and broad peaks similar to the first series indicating a meager electro catalytic activity of DLC based counter electrodes compared to ITO/Pt. In view of these results, the next series of counter electrodes are coated with a very small amount of Pt on top of N-doped DLC layer.

The third series of counter electrodes consisted of layered structure ITO/Cr/N-doped DLC/Pt. The N-doped DLC is deposited with 10 sccm of N_2 for 1.5 min similar to the best performed sample of first series, on which Pt is deposited by RF sputtering for 5, 10 s to give two counter electrodes in this series. The thicknesses of Pt layers were 6.25 nm (5 s) and 12.5 nm (10 s). For the fourth series, the ITO is replaced by glass plate and the deposition times of Pt are 2 & 3 min compared to third series of counter electrodes as given in Table 1. The small amounts of Pt and the use of glass plate instead of ITO are intended for decreasing the overall cost of the DSSC and also developing N-doped DLC as possible alternative to ITO/Pt counter electrodes.

The photovoltaic parameters using ITO/Cr/DLC (n-type)/Pt and Glass/Cr/DLC (n-type)/Pt as counter electrodes in the DSSCs are presented in Table 5. The conversion efficiencies of both the third series (with thin Pt layers) and the fourth series (with glass as substrate instead of ITO) are higher than the first and second series of counter electrodes studied in this work. A thin layer of Pt on ITO/Cr/DLC (n-type) has almost doubled its conversion efficiency. The ITO/Cr/DLC

Table 4
Photovoltaic parameters of DSSCs using ITO/Cr/DLC as the counter-electrodes.

Counter-electrode	Short circuit current I_{sc} (mA)	Open-circuit voltage V_{oc} (V)	Fill factor (FF)	Conversion efficiency (η)
ITO/Pt (standard cell)	2.70	0.65	0.46	3.20%
ITO/Cr/DLC (5 min)	1.60	0.58	0.35	1.30%
ITO/Cr/DLC (10.5 min)	1.92	0.59	0.35	1.57%
ITO/Cr/DLC (12 min)	1.59	0.58	0.24	0.90%

Note: ITO represents indium-tin-oxide coated glass substrates.

Table 5

Photovoltaic parameters of DSSCs using ITO/Cr/DLC (n-type)/Pt and Glass/Cr/DLC (n-type)/Pt as counter-electrodes.

Counter electrode	Short circuit current I_{sc} (mA)	Open-circuit voltage V_{oc} (V)	Fill factor (FF)	Conversion efficiency (η)
ITO/Pt (standard cell)	2.70	0.65	0.46	3.20%
ITO/Cr/DLC (N10)/Pt (5 s)	2.06	0.64	0.49	2.81%
ITO/Cr/DLC (N10)/Pt (10 s)	2.66	0.64	0.48	3.35%
Glass/Pt	2.26	0.60	0.46	2.55%
Glass/Cr/N10 DLC/Pt (2 min)	2.38	0.63	0.52	3.21%
Glass/Cr/N10 DLC/Pt (3 min)	2.40	0.66	0.48	3.10%

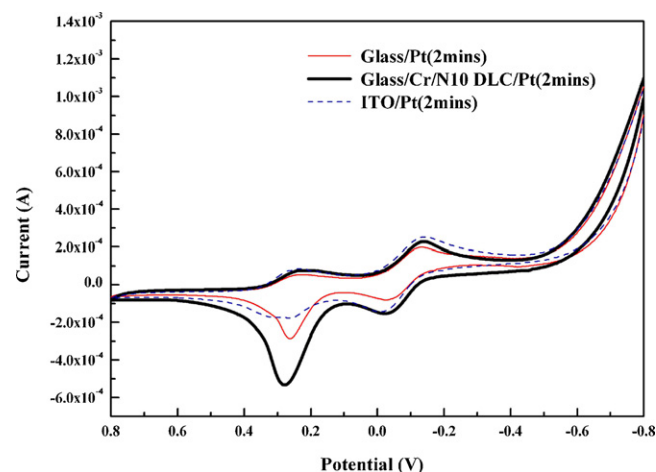
Note: ITO represents indium-tin-oxide coated glass substrates.

(n-type)/Pt-10 s counter electrode has demonstrated the best efficiency of 3.35% among all the electrodes studied in this report and is more than the conversion efficiency of standard ITO/Pt which has 3.20%. It means that the 150 nm thick Pt layer used in the standard counter electrode can be compensated by DLC and 12.5 nm thick Pt layer for higher performance. When the ITO is replaced by glass plate, the conversion efficiency was equally impressive with Glass/Cr/N10 DLC/Pt (2 min) showing 3.21% and Glass/Cr/N10 DLC/Pt (2 min) showing 3.10%. Though the thickness of Pt layer is more in the glass plate based counter electrodes compared to ITO based electrodes, the conversion efficiencies have been remarkably retained. Even for the Glass/Pt counter electrode the efficiency was higher than the first and second series of counter electrodes studied.

The sheet resistances of these counter electrodes are evaluated to understand their contribution for the conversion efficiency. The corresponding resistivity data for the counter electrodes of third and fourth series are presented in Table 6. The sheet resistivity has decreased a little for the Pt layer coated third series of electrodes compared to the second series which has no Pt layer (ITO/Cr/N10 DLC). The coating time of Pt also showed some difference in resistivity, because the distribution of Pt would be more uniform for 10 s than 5 s of coating. However, their values are still more than the standard ITO/Pt electrode's resistivity. Though the resistivity has not declined much, the catalytic activity for the redox reactions due to the small Pt layers must have contributed to the significant improvement of their conversion efficiencies.

In the glass substrate based electrodes, simple Glass/Pt has a sheet resistivity of 2.51 Ω/sq and Glass/Cr/N10 DLC has 39.48 Ω/sq . After depositing Pt layers on Glass/Cr/N10 DLC, the sheet resistance drastically reduces to even less than that of Glass/Pt. This implies that the thickness of Pt has a direct effect on sheet resistivity of the counter electrode. Fang et al. [30] also observed a decrease of sheet resistance with increase of Pt thickness from 2 to 415 nm in their counter electrode preparation. However, the catalytic activity for the Pt layer deposited for 2 min might have been better so the conversion efficiency for Glass/Cr/N10 DLC/Pt (2 min) is slightly more than Glass/Cr/N10 DLC/Pt (3 min) counter electrode.

The catalytic activity of Pt also depends on the underlying layers of Pt in the counter electrode. A comparison of CV curves for counter electrodes Glass/Pt, Glass/Cr/N10 DLC/Pt and ITO/Pt

**Fig. 4.** Cyclic voltammograms for the Glass/Pt, Glass/Cr/DLC the (n-type)/Pt (2 min) and ITO/Pt electrodes.

is made in Fig. 4 with Pt being deposited for 2 min in all cases. The anodic and cathodic peaks of Glass/Cr/N10 DLC/Pt are clear and strong with more peak height and area indicating better catalytic activity. Glass/Pt and ITO/Pt have nearly similar profiles. From these results, it's clear that a layer of N-doped DLC has a significant effect on catalysis of redox reactions at counter electrode. Among the Glass and ITO substrates, since the resistivity is more for Glass/Pt (2.51 Ω/sq) compared to ITO/Pt (1.50 Ω/sq), the conversion efficiency for ITO/Pt (3.20%) is better than Glass/Pt (2.55%) under these conditions. Therefore, both the catalytic activity and the sheet resistivity of the counter electrode are crucial for the overall performance of the DSSCs.

4. Conclusions

Attempts were made to use nitrogen-doped diamond like carbon (n-type DLC) as a counter electrode in place of Pt for the dye sensitized solar cell (DSSC). Four different series of counter electrode structures (ITO/Pt/DLC (n-type), ITO/Cr/DLC (n-type), ITO/Cr/DLC (n-type)/Pt, and Glass/Cr/DLC (n-type)/Pt) containing DLC are studied in a systematic procedure to understand the contribution of DLC towards the conversion efficiency of corresponding DSSCs. 10 sccm of N_2 concentration gave optimal doping and best conductivity for the DLC based counter electrode. The counter electrode ITO/Cr/DLC (n-type) gave a best conversion efficiency of 1.57% when the n-type DLC is deposited for 10.5 min. When a layer of Pt (12.5 nm thick) is coated on ITO/Cr/DLC (n-type) counter electrode, the conversion efficiency reached 3.35%, while standard ITO/Pt showed 3.20% conversion efficiency under similar conditions (100 mA/cm^2 intensity illumination). This is remarkable as it signifies the positive impact of n-type DLC interlayer for enhancement of conversion efficiency. Further, the replacement of ITO by glass plate and simultaneous increase of Pt layer thickness almost retained the conversion efficiency. In conclusion, nitrogen doped

Table 6

Sheet resistivity of counter-electrodes ITO/Cr/DLC (n-type)/Pt and Glass/Cr/DLC (n-type)/Pt.

Counter electrode	Sheet resistivity (Ω/sq)
ITO/Pt (standard cell)	1.50
ITO/Cr/N10 DLC	7.59
ITO/Cr/N10 DLC/Pt (5 s)	6.93
ITO/Cr/N10 DLC/Pt (10 s)	6.65
Glass/Pt	2.51
Glass/Cr/N10 DLC	39.48
Glass/Cr/N10 DLC/Pt (2 min)	2.25
Glass/Cr/N10 DLC/Pt (3 min)	1.33

Note: ITO represents indium-tin-oxide coated glass substrates.

DLC could compensate the Pt layer to some extent in normal counter electrodes of DSSC. It can also improve the conversion efficiency by utilizing a minimum amount of Pt in combination with it. A glass plate can be used as substrate instead of ITO for similar performance of counter electrode, when n-type DLC is used as interlayer.

References

- [1] M. Gratzel, J. Photochem. Photobiol. A 164 (2004) 3.
- [2] M.K. Nazeeruddin, A. Kay, I. Rodicio, R.H. Baker, E. Miiller, P. Liska, N. Vlachopoulos, M. Gratzel, J. Am. Chem. Soc. 115 (1993) 6382.
- [3] H. Lindstrom, A. Holmberg, E. Magnusson, S.E. Lindquist, L. Malmqvist, A. Hagfeldt, Nano Lett. 1 (2001) 97.
- [4] M. Okuya, K. Nakade, D. Osa, T. Nakano, G.R. Asoka Kumara, S. Kaneko, J. Photochem. Photobiol. A 164 (2004) 167.
- [5] W.J. Lee, D.Y. Lee, I.S. Kim, S.J. Jeong, J.S. Song, Trans. Elect. Electron. Mater. 6 (2005) 140.
- [6] Md.K. Nazeeruddin, F.D. Angelis, S. Fantacci, A. Selloni, G. Viscardi, P. Liska, S. Ito, B. Takeru, M. Graetzel, J. Am. Chem. Soc. 127 (2005) 16837.
- [7] Y. Chiba, A. Islam, Y. Watanabe, R. Komiya, N. Koide, L. Han, Jpn. J. Appl. Phys. 45 (2006) L638.
- [8] T.N. Murakami, M. Gratzel, Inorg. Chim. Acta 361 (2008) 572.
- [9] Z. Huang, X. Liu, K. Li, D. Li, Y. Luo, H. Li, W. Song, L.Q. Chen, Q. Meng, Electrochem. Commun. 9 (2007) 596.
- [10] T.N. Murakami, S. Ito, Q. Wang, Md.K. Nazeeruddin, T. Bessho, I. Cesar, P. Liska, R.H. Baker, P. Comte, P. Pechy, M. Gratzel, J. Electrochem. Soc. 153 (2006) A2255.
- [11] E. Ramasamy, W.J. Lee, D.Y. Lee, J.S. Song, Electrochem. Commun. 10 (2008) 1087.
- [12] Y. Saito, T. Kitamura, Y. Wada, S. Yanagida, Chem. Lett. 31 (2002) 1060.
- [13] Y. Saito, W. Kubo, T. Kitamura, Y. Wada, S. Yanagida, J. Photochem. Photobiol. A. Chem. 164 (2004) 153.
- [14] N. Ikeda, K. Teshima, T. Miyasaka, Chem. Commun. 2006 (2006) 1733.
- [15] J.G. Chen, H.Y. Wei, K.C. Ho, Sol. Energy Mater. Sol. Cells 91 (2007) 1472.
- [16] A. Grill, Diamond Relat. Mater. 8 (1999) 428.
- [17] W. Kulisch, Deposition of Superhard Diamond-Like Materials, Springer, Heidelberg, 1999.
- [18] G. Lazar, I. Lazar, J. Non-Cryst. Solids 331 (2003) 70.
- [19] N.E. Derradji, M.L. Mahdjoubi, H. Belkhir, N. Mumumbila, B. Angleraud, P.Y. Tessier, Thin Solid Films 482 (2005) 258.
- [20] W. Zhang, Y. Xia, J. Ju, L. Wang, Z. Fang, M. Zhang, Solid State Commun. 126 (2003) 163.
- [21] F. Alibert, O.D. Drouhin, M. Lejeune, M. Benlarsen, S.E. Rodil, E. Camps, Diamond Relat. Mater. 17 (2008) 925.
- [22] V.G. Litovchenko, N.I. Klyui, Sol. Energy Mater. Sol. Cells 68 (2001) 55.
- [23] Z.B. Zhou, R.Q. Cui, Q.J. Pang, G.M. Hadi, Z.M. Ding, W.Y. Li, Sol. Energy Mater. Sol. Cells 70 (2002) 487.
- [24] M. Umeno, S. Adhikary, Diamond Relat. Mater. 14 (2005) 1973.
- [25] S.F. Wang, J.C. Pu, J.C. Sung, Thin solid films, [in press](#).
- [26] A. Luque, S. Hegedus (Eds.), Hand book of Photovoltaic Science and Engineering, John Wiley & Sons, 2003.
- [27] P. Li, J. Wu, J. Lin, M. Huang, Z. Lan, Q. Li, Electrochim. Acta 53 (2008) 4161.
- [28] K. Suzuki, M. Yamaguchi, M. Kumagai, S. Yanagida, Chem. Lett. 32 (2003) 28.
- [29] K.J. Hansen, C.W. Tobias, J. Electrochem. Soc. 134 (1987) 2204.
- [30] X. Fang, T. Ma, G. Guan, M. Akiyama, T. Kida, E. Abe, J. Electroanal. Chem. 570 (2004) 257.
- [31] P. Stumm, D.A. Drabold, P.A. Fedder, J. Appl. Phys. 81 (1997) 1289.